Biochemical Pharmacology, Vol. 37, No. 13, pp. 2575–2583, 1988.
Printed in Great Britain.

0006-2952/88 $3.00 + 0.00

CHARACTERIZATION OF CHOLINERGIC MUSCARINIC RECEPTORS IN THE RABBIT IRIS

RICHARD E. HONKANEN and ATA A. ABDEL-LATIF*
Department of Cell and Molecular Biology, Medical College of Georgia, Augusta, GA 30912-2100, U.S.A.

(*Received* 3 *August* 1987; *accepted* 30 *November* 1987)

Abstract—The sphincter smooth muscle of the iris is innervated by excitatory parasympathetic nerve fibers, and the activation of these fibers results in the breakdown of phosphatidylinositol 4,5-bisphosphate into its derived second messengers, myosin light chain phosphorylation and muscle contraction. The present study characterizes the muscarinic acetylcholine receptors (mAChRs) of the rabbit iris employing [^{3}H]*N*-methylscopolamine ([^{3}H]NMS) and L-[^{3}H]quinuclidinyl benzilate ([^{3}H]QNB) as probes. Binding studies indicated that [^{3}H]NMS and [^{3}H]QNB bound to homogeneous populations of mAChRs with apparent B_{max} values of 0.67 and 1.09 pmol/mg protein respectively. Binding of radioligands was rapid, saturable, stereospecific, reversible, and inhibited by specific muscarinic agonists and antagonists in a competitive manner. [^{3}H]NMS displayed a lower amount of nonspecific binding and a faster association and dissociation rate than [^{3}H]QNB. The relative potencies for displacement of both radioligands, based on their K_i values, were (−)QNB > atropine> (+)QNB > pirenzepine > pilocarpine. Antagonist displacement of the radioligands appeared to obey the law of mass action, indicating interaction with a single binding site. However, displacement of the radioligands by the agonists carbamylcholine and methacholine indicated interaction with both high and low affinity binding sites. Comparison of the displacement of [^{3}H]NMS and [^{3}H]QNB by pirenzepine in microsomal fractions from rabbit iris, ileal muscle and cerebral cortex revealed the presence of a single subtype of mAChR in the iris which had an affinity for PZ that was slightly higher than that of ileal M_2 receptors, but lower than that of brain M_1 receptors. This suggests that the mAChRs in the iris may represent a subclass of receptors within the M_2 subtype, or they may constitute an entirely different subtype of mAChRs.

Although the ocular hypotensive effects of cholinergic antiglaucoma drugs have been well characterized, little is known about the molecular basis of their actions [1, 2]. In a variety of tissues, muscarinic agents mediate a number of cellular responses including polyphosphoinositide breakdown, inhibition of adenylate cyclase, arachidonate release, and modulation of potassium channels [3–6]. While these cellular events were initially thought to be mediated through the actions of a single type of muscarinic receptor, recent studies with the atypical muscarinic antagonist, pirenzepine, provide convincing evidence for the subclassification of muscarinic acetylcholine receptors (mAChRs†) into M_1 (high affinity for pirenzepine) and M_2 (low affinity for pirenzepine) subtypes [7–9]. Additional support for the subclassification of mAChRs comes from molecular studies which indicate that the M_1 and M_2 subtypes represent distinct gene products, and as many as four types of mAChRs are present in the rat cerebral cortex [10–12, see also Ref. 36 below]. Nonetheless, it is still not clear if a particular physiological response, such as polyphosphoinositide breakdown or adenylate cyclase inhibition, is linked to a specific receptor subtype.

The iris of the eye is innervated by both parasympathetic and sympathetic nerves. The sphincter muscle is innervated parasympathetically via the ocular motor nerve, and the dilator muscle is innervated sympathetically via the superior cervical ganglion. The sphincter responds to muscarinic agonists and antagonists in a characteristic manner: agonists cause miosis, whereas antagonists cause mydriasis. In the iris, acetylcholine induces several physiological responses including control of sphincter smooth muscle contraction, polyphosphoinositide breakdown, arachidonate release, prostaglandin synthesis, and myosin light chain phosphorylation [13–16]. Correlative studies on the effect of time, temperature, Ca^{2+} and atropine antagonism on carbachol-induced inositol triphosphate accumulation, muscle contraction and myosin light chain phosphorylation suggest that there is a close relationship between the pharmacological and biochemical responses in the iris smooth muscle [14, 15]. However, although muscarinic receptors have been identified in the iris via binding studies with [^{3}H]quinuclidinylbenzilate [17–19] and autoradiography [20], their detailed characterization and subclassification into subtypes have not yet been performed.

To gain further insight into the molecular events initiated by cholinergic agents in the iris, a better understanding of mAChR subtypes is essential. As

* Author to whom correspondence should be addressed.

† Abbreviations: mAChR, muscarinic acetylcholine receptor; [^{3}H]QNB, L-[^{3}H]quinuclidinyl benzilate; [^{3}H]NMS, [^{3}H]*N*-methylscopolamine; AFDX-116, 11-[[2-[(diethylamino)methyl] - 1 - piperidinyl]acetyl] - 5,11 - dihydro - 6*H* - pyrido-[2,3 - b][1,4]benzodiazepine - 6 - one; and HEPES, *N*-2-hydroxyethylpiperazine-*N'*-2-ethanesulfonic acid.

part of a study on the role of polyphosphoinositides and their derived second messengers in the mechanism of cholinergic desensitization of the iris [21], we have characterized the mAChRs of the rabbit iris based on the interactions of a variety of muscarinic agents with membrane binding sites identified with [^{3}H]*N*-methylscopolamine ([^{3}H]NMS) and L-[^{3}H]quinuclidinylbenzilate ([^{3}H]QNB). Our studies indicate the prevalence of a single subtype of muscarinic receptor in the iris which has an affinity for pirenzepine that is somewhat higher than that of the ileal smooth muscle M_2 receptor but lower than that of brain M_1 receptor.

METHODS

Preparation of microsomal fractions from rabbit iris

Tissues for the following experiments were obtained from albino rabbits at a local slaughterhouse. Eyes were enucleated immediately after killing and transported to the laboratory packed in ice. The methods of homogenization, subcellular fractionation, and assessing the purity of the microsomal preparations were essentially the same as described previously [19]. Briefly, approximately 5–15 g (wet wt) of irides were rinsed with ice-cold incubation buffer (142 mM NaCl, 5.6 mM KCl, 2.2 mM $CaCl_2$, 3.6 mM $NaHCO_3$, 1.0 mM $MgCl_2$, 5.6 mM glucose, 30 mM HEPES, pH 7.4 with NaOH), blotted gently, and placed in 5 ml of sucrose buffer (300 mM sucrose, 1.0 mM EDTA, 10 mM Tris base, pH 7.4 with concentrated HCl). The muscles were minced with scissors, suspended in 10 vol. of sucrose buffer, and homogenized for 4 × 30 sec with a Super Dispax tissumizer model SDT-182 (Tekmar Co.) at 2/3 maximum speed. The homogenate was filtered through cheesecloth and centrifuged at 1200 *g* for 20 min. The resultant supernatant fraction was spun at 10,000 *g* for 30 min to pellet the mitochondrial fraction, and the supernatant from the mitochondrial pellet was then centrifuged at 100,000 *g* for 90 min to sediment the microsomal fraction. The microsomal fraction was resuspended in incubation buffer to a concentration of 1.0 mg protein/ml and either used immediately or divided into 0.5-ml aliquots and snap frozen in liquid nitrogen for storage at −70°. Microsomal fractions from ileal smooth muscle and cerebral cortex were prepared essentially in the same manner. Protein was determined by the method of Bradford [22] with bovine serum albumin as a standard.

Binding of [^{3}H]*NMS and* [^{3}H]*QNB*

The binding of radioligands to iris microsomal muscarinic receptors was assayed by a modification of the procedures of Yamamura and Snyder [23].

Saturation experiments. Iris microsomes (50–100 μg protein) were incubated in 2.5 ml of incubation buffer along with different concentrations of [^{3}H]NMS or [^{3}H]QNB at 37°. Reactions were terminated after 60 min by vacuum filtration through glass fiber filters (Schleicher and Schuell No. 32) using a Brandell cell harvester, and the filters were immediately washed three times with 6 ml of rinse solution. Individual filters were then allowed to air dry overnight and placed in vials containing 8 ml of scintillation fluid for >12 hr prior to counting. Radioactivity was determined with a Beckman LS-7500 scintillation counter, and quench corrections were performed. Binding reactions were performed in either triplicate or duplicate together with duplicate samples containing 5 μM atropine to estimate nonspecific binding. The number of ligand binding sites was determined with a weighted nonlinear least square regression analysis of the binding data as described by Munson and Rodbard [24]. When the data statistically best fit a one-site model, a least square linear regression analysis of the Scatchard [25] and Hill [26] transformations of the data was used to estimate maximum binding (B_{max}), receptor–ligand dissociation constants (K_D) and "goodness" of fit to the model. In some experiments, where a significant amount of the total radiolabeled ligand added to the incubation solution was bound (i.e. experiments conducted with low concentrations of ligands), the volume of the incubation solution was increased until >95% of the radioactivity originally added remained in solution after equilibrium conditions were reached.

Competitive binding experiments. Iris microsomes (50 μg protein) were incubated with 0.10 ± 0.025 nM (mean ± SE) [^{3}H]NMS or [^{3}H]QNB in the absence and presence of increasing amounts of unlabeled muscarinic agonists or antagonists. The incubation and rinsing conditions were the same as described above, and the binding data were analyzed to obtain binding affinity and receptor density by iterative non-linear least square curve-fitting procedures [24]. Complex ligand–receptor systems were analyzed with the computer program "Ligand" as described by Munson and Rodbard [24] to determine ligand dissociation and inhibition constants. Such data analysis assumes a one-, two-, or three-site receptor, and the differences in fits of experimental data were compared with the three models to statistically (F-test) assess the "goodness of fit." The simplest model which offered a good statistical fit was used to interpret the data.

Dissociation experiments. Equilibrium was attained by incubating microsomes (50 μg protein) in 2.5 ml of incubation buffer with radiolabeled ligand at a concentration $\sim = K_D$ of the ligand (K_D for [^{3}H]NMS = 2.4×10^{-10} M, K_D for [^{3}H]QNB = 3.9×10^{-11} M) for 60 min at 37°. Ligand dissociation was initiated by the addition of an excess concentration (10.0 μM) of unlabeled atropine. The reaction was stopped at various time intervals by vacuum filtration, and the filters were washed three times with 6 ml of incubation buffer as described above. Nonspecific binding was determined by including 10.0 μM atropine in the incubation medium of some assays. Dissociation experiments were conducted in duplicate and repeated three or more times. The data was plotted as percent specific binding versus time after the addition of 10.0 μM atropine. The dissociation curves were then analyzed with a weighted non-linear curve-fitting technique [24, 27] to determine if dissociation data best fit a mono- or bi-exponential model. The dissociation rate constants (K_{-1}) were then calculated according

to the following expression:

$$[Rbt] = \sum_{i=1}^{i=n} [Roi] \cdot e^{(-k_{-1i} \cdot t)}$$

where $[Rbt]$ is the amount of radioligand bound at time t, $[Ro]$ is the amount bound at time = 0 and k_{-1} is the dissociation rate constant for each site i out of a possible n sites.

Association experiments. Iris microsomes (50 μg protein) were incubated at 37° in incubation buffer (see above) with [^{3}H]NMS or [^{3}H]QNB at a concentration equal to the K_D of the labeled ligand in a final volume of 2.5 ml. The reaction was stopped at different time intervals by vacuum filtration, rinsed, counted and corrected for nonspecific binding as described above. The observed association rate constant $K_{(obs)}$ was then calculated according to the following equation:

$$[Rbt] = \sum_{i=1}^{i=n} [RE_i] \cdot (1 - e^{(-K_{(obs)i} \cdot t)})$$

where RE_i is the amount of radioligand bound at equilibrium and $K_{(obs)}$ is the observed association constant of site i out of a possible n sites. $K_{(obs)}$ is then related to the actual association rate constant (k_{+1}) through the following equation:

$$k_{+1i} = \frac{K_{(obs)} - k_{-1i}}{[L]}$$

where L is the concentration of radioligand and k_{-1} is the dissociation constant for site i as determined above.

Materials

This L-isomer of [^{3}H]QNB (46 Ci/mmol) and [^{3}H]NMS (72 Ci/mmol) were obtained from Amersham (Arlington Heights, IL). Other drugs used in the present study included carbachol (carbamylcholine), atropine sulfate, methacholine and pilocarpine (Sigma Chemical Co., St. Louis, MO); oxotremorine (Aldrich Chemical Co., Milwaukee, WI); and (−)QNB and (+)QNB (Research Biochemicals, Inc., Natick, MA). Pirenzepine dihydrochloride was a gift from Boehringer Ingelheim Pharmaceuticals, Inc. (Ridgefield, CT). All other chemicals were reagent grade.

RESULTS

Binding of [^{3}H]*NMS and* [^{3}H]*QNB to iris microsomes*

The specific binding of both [^{3}H]NMS and [^{3}H]QNB to rabbit iris microsomes demonstrated saturability with maximum specific binding obtained at a concentration of about 1.0 nM (Fig. 1). Upon saturation, the specific binding of [^{3}H]NMS was about 61% of that of [^{3}H]QNB with an apparent maximal number of binding sites (B_{max}) determined to be 0.67 and 1.09 pmol/mg protein respectively. Scatchard analysis of the saturation isotherms (Fig. 1) indicated that both ligands bound with high affinity, having apparent dissociation constants (K_D) of 2.4×10^{-10} and 3.9 ± 10^{-11} M for [^{3}H]NMS and [^{3}H]QNB respectively. This suggests that [^{3}H]QNB binds iris microsomal receptors with a slightly greater affinity than [^{3}H]NMS. Both Scatchard and Hill plots of binding data were linear, and Hill coefficients of 1.0 for [^{3}H]NMS and 0.94 for [^{3}H]QNB specific binding indicate that both radioligands interacted with a homogeneous population of muscarinic receptors in the iris.

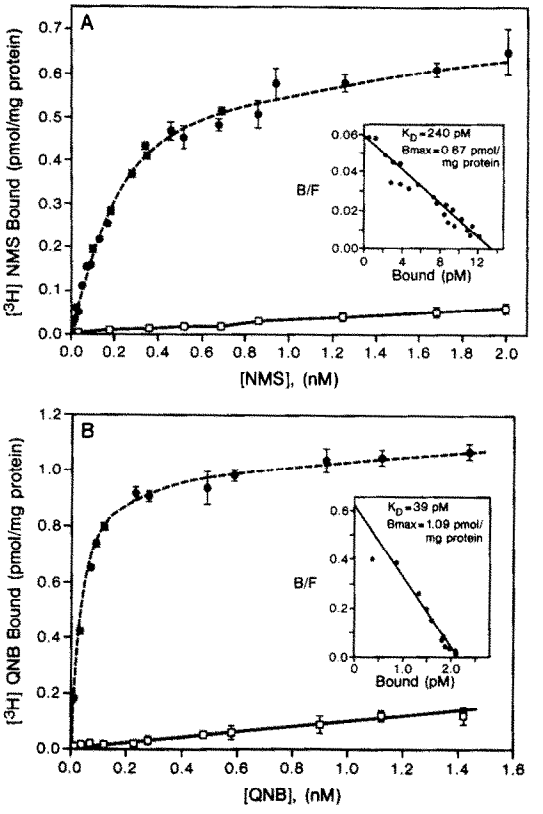

Fig. 1. Specific binding of [^{3}H]NMS (A) and [^{3}H]QNB (B) to rabbit iris microsomes as a function of ligand concentration. Key: (●) specific binding; (□) nonspecific binding. Insets: Scatchard plots of the binding data. Saturation experiments were performed as described in Methods, and nonspecific binding was estimated with the addition of 5 μM atropine to the incubation medium. Each point represents the mean ± SEM of six determinations.

Association and dissociation kinetics of [^{3}H]*NMS and* [^{3}H]*QNB binding*

The association and dissociation rate curves of [^{3}H]NMS and [^{3}H]QNB specific binding to the microsomal fraction of the iris are shown in Figs. 2 and 3. In association experiments, [^{3}H]NMS binding increased rapidly with time for about 15 min and then plateaued, indicating that a steady-state binding equilibrium had been reached (Fig. 2A). Once equilibrium binding was achieved, no further change in binding was observed over a period of >120 min. The rate of [^{3}H]QNB binding was similar to that of [^{3}H]NMS except that equilibrium binding conditions were not reached for about 40 min (Fig. 2B). Weighted non-linear regression analysis of the association curves for both [^{3}H]NMS and [^{3}H]QNB binding best fit a one-site model with association rate

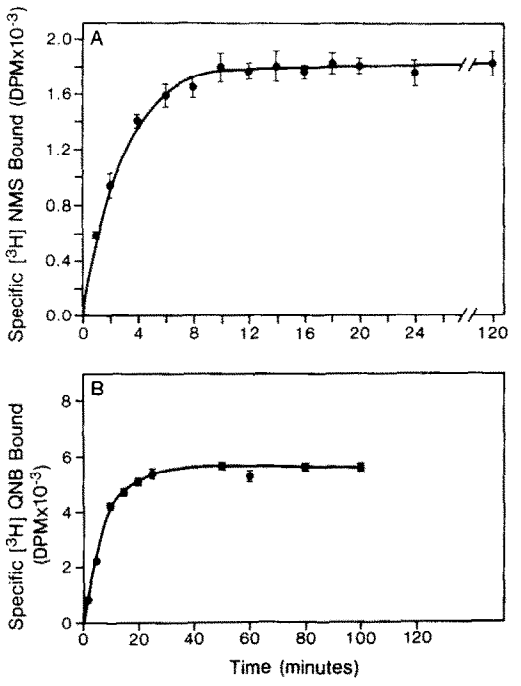

Fig. 2. Time course for the association of [^{3}H]NMS (A) and [^{3}H]QNB (B) binding to iris microsomes. Microsomes were incubated with 240 pM [^{3}H]NMS or 39 pM [^{3}H]QNB (this concentration represents the apparent dissociation constants for NMS and QNB) for various time intervals as indicated, and the reactions were stopped by vacuum filtration as described under Methods. Each point represents the mean ± SEM of six determinations.

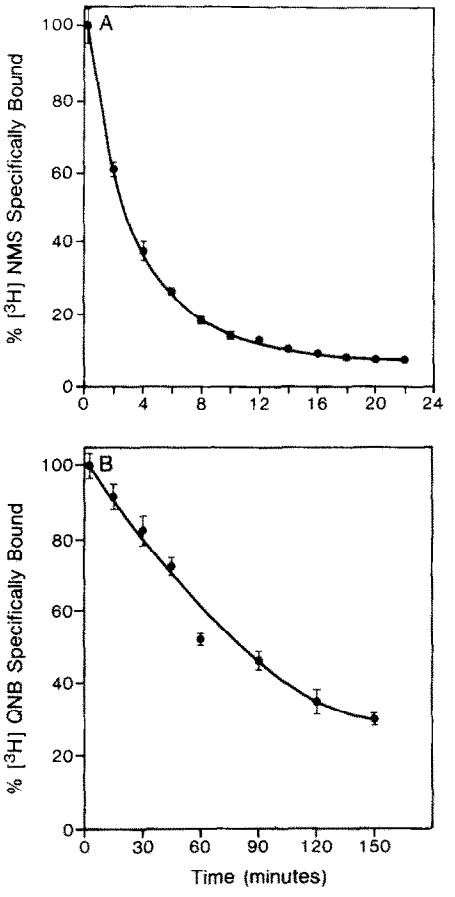

Fig. 3. Time course for the dissociation of [^{3}H]NMS (A) and [^{3}H]QNB (B) from iris microsomes. Microsomes were incubated with 240 pM NMS and 39 pM QNB for 60 min. Dissociation was started by adding 10 μM atropine, and the reactions were stopped at various time intervals as indicated by vacuum filtration. Each point represents the mean ± SEM of six determinations.

constants (k_{+1}) of 1.19×10^9 and 2.26×10^7 M^{-1} min^{-1} respectively.

The reversibility of ligand binding was readily demonstrated in dissociation experiments (Fig. 3). In the presence of excess atropine (10 μM), bound [^{3}H]NMS (Fig. 3A) or [^{3}H]QNB (Fig. 3B) dissociated steadily with time. The $T_{\frac{1}{2}}$ values for dissociation of [^{3}H]NMS and [^{3}H]QNB were found to be 2.75 and 83 min respectively. Non-linear regression analysis of the dissociation curves showed that [^{3}H]QNB dissociation best fit a monophasic model with a dissociation rate constant (k_{-1}) determined to be $9.02 \times 10^{-3} \pm 5.3 \times 10^{-4}$ min^{-1}. [^{3}H]NMS dissociation best fit a biphasic model having dissociation rate constants of 0.62 ± 0.01 and 0.323 ± 0.03 min^{-1} for the slow and fast components respectively.

Inhibition of [^{3}H]*NMS and* [^{3}H]*QNB specific binding by muscarinic antagonists*

Selected muscarinic antagonists were tested for their potency in inhibiting [^{3}H]NMS and [^{3}H]QNB specific binding to iris microsomes (Fig. 4). Inhibition of radioligand binding by muscarinic antagonists occurred in a dose-dependent manner, and complete inhibition was obtained with all antagonists tested. The relative potencies for antagonist displacement of [^{3}H]NMS (Fig. 4A) and [^{3}H]QNB (Fig. 4B) were similar with a rank order, based on the K_i values of the antagonists, as follows: (−)QNB > atropine > (+)QNB > pirenzepine > pilocarpine. Pilocarpine, which is a partial agonist in some tissues, does not induce a contractile response in the rabbit iris [28]. In fact, pilocarpine markedly antagonizes the effects of carbachol in the iris [29], and thus was included with the antagonists in the present study. Stereoselective binding was demonstrated with the (+) and (−) enantiomers of QNB where the inhibitory effect of the latter was over 100-fold greater than that of the former (Fig. 4). Antagonist displacement curves of both [^{3}H]NMS and [^{3}H]QNB were steep, and analysis of the displacement curves for all the muscarinic antagonists tested best fit a one-site model. Thus, muscarinic antagonist displacement of both [^{3}H]NMS and [^{3}H]QNB from microsomal receptors of the rabbit iris appears to be in accordance with the law of mass action.

Inhibition of [^{3}H]*NMS and* [^{3}H]*QNB specific binding by muscarinic agonists*

Selected muscarinic agonists were tested for their potency in inhibiting [^{3}H]NMS and [^{3}H]QNB specific

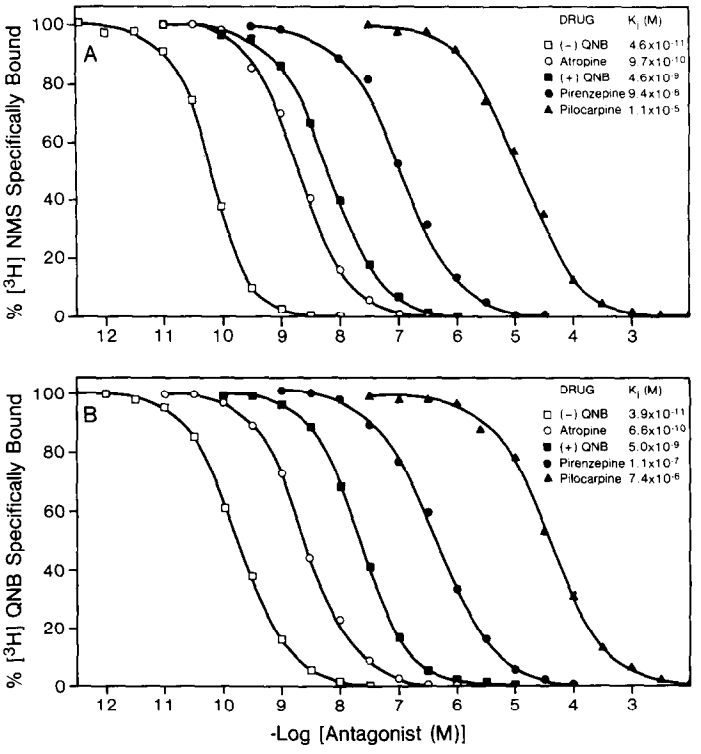

Fig. 4. Displacement of specific [^{3}H]NMS (A) and [^{3}H]QNB (B) binding in rabbit iris microsomes by selected muscarinic antagonists. Microsomes (50 μg protein) were incubated for 60 min at 37° with 0.1 nM [^{3}H]NMS or [^{3}H]QNB and various concentrations of antagonists in 2.5 ml of buffer. Reactions were stopped by vacuum filtrations as described in Methods. Each point represents the mean of six to twelve determinations.

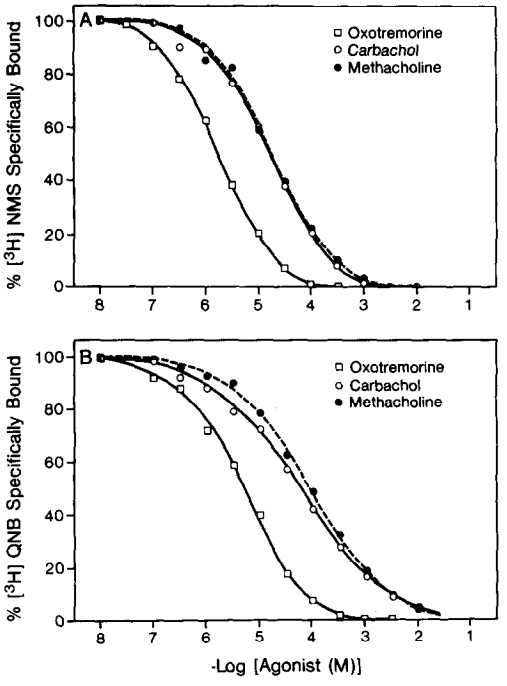

Fig. 5. Displacement of specific [^{3}H]NMS (A) and [^{3}H]QNB (B) binding in rabbit iris microsomes by selected muscarinic agonists. Assays were conducted as described in the legend of Fig. 4 and Methods. Each point represents the mean of six to twelve determinations.

binding to iris microsomes (Fig. 5). Muscarinic agonists were less potent than antagonists at displacing [^{3}H]NMS (Fig. 5A) and [^{3}H]QNB (Fig. 5B), and analysis of agonist displacement curves showed that carbachol and methacholine best fit a two-site model, whereas oxotremorine best fit a one-site model (Table 1). Further analysis of the displacement data indicated that the high affinity components of carbachol and methacholine binding were similar, having estimated equilibrium dissociation constants ranging between 1.4 and 5.9 μM. The low affinity components had equilibrium dissociation constants that varied considerably, ranging from 79 to 240 μM. However, it should be noted that both (+) and (−) isomers of methacholine were present in this experiment; this may account for the inconsistencies in the percentages of high and low affinity binding sites obtained when different radioligands were used (Table 1). The displacement curves of both [^{3}H]NMS and [^{3}H]QNB by oxotremorine were similar, indicating the presence of a single binding site with a K_D of about 1.5 μM (Table 1).

Comparison of atropine and pirenzepine displacement of [^{3}H]NMS and [^{3}H]QNB specific binding to microsomes from rabbit cerebral cortex, ileum, and iris

The muscarinic antagonist, pirenzepine, is capable of distinguishing between M_1 and M_2 muscarinic receptor subtypes by binding to the M_1 subtype with

Table 1. Comparison of estimates from a two-site binding model for the inhibition of [^{3}H]NMS and [^{3}H]QNB binding to rabbit iris microsomes by selected muscarinic agonists

Agonist	[^{3}H]NMS				[^{3}H]QNB			
	K_H (μM)	K_L (μM)	% R_H	% R_L	K_H (μM)	K_L (μM)	% R_H	% R_L
Carbachol	5.9	79	70.0	29.9	2.9	110	50.1	49.9
Methacholine	1.4	240	35.4	64.5	4.1	120	45.9	54.1
Oxotremorine	1.6		100	0	1.5		100	0

The agonist displacement curves shown in Fig. 5 were analyzed with the computer program "Ligand" as described in Methods. K_H and K_L represent the estimated dissociation constants for the high and low affinity binding sites respectively. % R_H and % R_L represent the percentages of high and low affinity sites respectively.

a higher affinity than it binds to the M_2 subtype [7–9]. To determine the subtype(s) of muscarinic receptors in the iris, we compared the inhibition of [^{3}H]NMS and [^{3}H]QNB binding by pirenzepine and atropine in microsomes from the ileum, which contains almost exclusively the M_2 subtype [7], the cerebral cortex, which contains predominantly the M_1 subtype [30–32], and the iris (Fig. 6). Although the inhibition curves for the displacement of [^{3}H]QNB were located slightly to the right of those for [^{3}H]NMS, which can be accounted for by the use of 0.1 nM solutions of [^{3}H]NMS or [^{3}H]QNB in the assays while the apparent K_D of [^{3}H]QNB was lower than that of [^{3}H]NMS, the pirenzepine and atropine

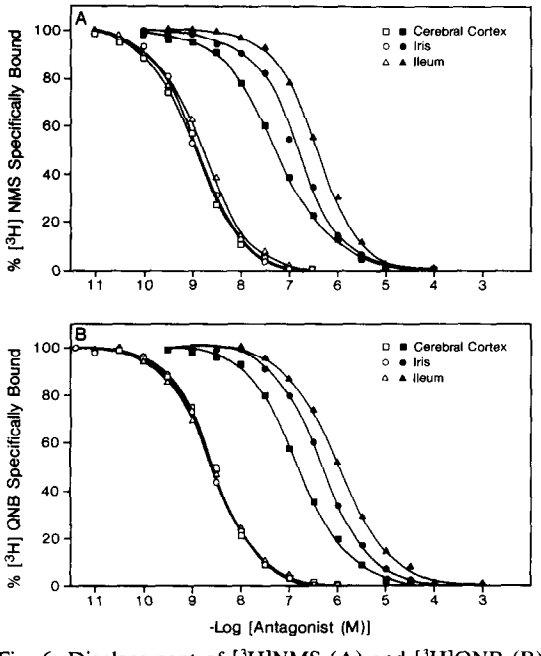

Fig. 6. Displacement of [^{3}H]NMS (A) and [^{3}H]QNB (B) binding by atropine (open symbols) and pirenzepine (closed symbols) in microsomes prepared from rabbit cerebral cortex, ileum smooth muscle and iris smooth muscle. Conditions of incubation and methods of analysis were the same as described in the legend of Fig. 4, and each point represents the mean of twelve to twenty-four determinations.

displacement patterns of the two radioligands were similar. Non-linear regression analysis of the data showed that in all three tissues the displacement of both radioligands by atropine best fit a one-site model with a K_i ranging from 6.4×10^{-10} to 9.9×10^{-10} M (Table 2). Similarly, analysis of the pirenzepine displacement data from ileal and iris smooth muscle microsomes also best fit a one-site model, indicating that only a single binding site could be detected. Analysis of the data obtained from the cerebral cortex best fit a two-site model (Table 2). In cerebral cortex microsomes, about 77 and 84% of the [^{3}H]NMS and [^{3}H]QNB binding sites, respectively, had a high affinity for pirenzepine, suggesting that they are of the M_1 receptor subtype. The remainder of the mAChRs in the cerebral cortex, and all of those in the ileal smooth muscle, had a relatively low affinity for pirenzepine that is characteristic of the M_2 receptor subtype. In the iris, although analysis of the data suggested the presence of a single binding site for pirenzepine, the mAChRs of this tissue had a higher affinity for pirenzepine than did those of the ileal smooth muscle (Fig. 6, Table 2). Thus, the mAChRs in the iris may represent a subclass of receptors within the M_2 subtype or they may constitute an entirely different subtype of mAChR.

DISCUSSION

The present data on the characterization of [^{3}H]NMS and [^{3}H]QNB binding to rabbit iris microsomes (summarized in Table 3) are typical for the binding of these radioligands to mAChRs; binding was saturable, stereospecific, of high affinity and inhibited by specific muscarinic agonists and antagonists. The binding of radioligands was proportional to the amount of protein added to the assay (data not shown) and displayed a very favorable specific to nonspecific binding ratio (Fig. 1). Scatchard plots of saturation isotherms for [^{3}H]NMS and [^{3}H]QNB specific binding were linear and had Hill coefficients that were close to unity, indicating that the interaction of both ligands occurs with a homogeneous population of mAChRs.

In the iris, [^{3}H]NMS bound about 61% of the binding sites identified with [^{3}H]QNB binding which is similar to that reported in heart, cerebral cortex, hippocampus, cerebellum and brain stem [33]. The

Table 2. Comparison of estimates from one- and two-site binding models for the displacement of [^{3}H]NMS and [^{3}H]QNB binding to rabbit cerebral cortex, ileum smooth muscle and iris smooth muscle microsomes by atropine and pirenzepine

Tissue	Displacer	[^{3}H]NMS						[^{3}H]QNB					
		K_i (nM)	K_L (nM)	K_H (nM)	% R_H	% R_L	IC_{50} (nM)	K_i (nM)	K_L (nM)	K_H (nM)	% R_H	% R_L	IC_{50} (nM)
Cortex*	Atropine	0.96					2.3 ± 0.1	0.64					2.8 ± 0.12
	Pirenzepine		670	28	77.3	22.7	61 ± 5.1		460	32	83.7	16.2	120 ± 9.1
Ileum	Atropine	0.99					1.8 ± 0.3	0.66					2.9 ± 0.02
	Pirenzepine	300					450 ± 39	254					980 ± 40
Iris*	Atropine	0.98					1.4 ± 0.1	0.66					2.7 ± 0.16
	Pirenzepine	110					160 ± 9.4	140					540 ± 44

The antagonist displacement curves shown in Fig. 6 were analyzed with the computer program "Ligand" as described in Methods. K_i represents the inhibition constant when the competition curves best fit a one-site model, and K_H and K_L represent the dissociation constants for the high affinity and low affinity sites when the curves best fit a two-site model. The IC_{50} values represent drug concentrations that produce 50% inhibition of specific ligand binding; each value represents the mean ± SE, N = 6.

*Presented as a poster at a symposium on Regulation of the Transport Mechanisms sponsored by the Biophysical Society, September 27–30, 1987, at the Duke University Marine Laboratory at Beaufort, NC.

binding of [^{3}H]NMS to a subpopulation of [^{3}H]QNB binding sites could be due to an easier access of the more hydrophobic QNB molecule to inactive or internalized receptors; such receptors may not be accessible to NMS due to its charged quaternary nitrogen [33–35]. In general, NMS was less hydrophobic, displayed lower nonspecific binding, and had a faster association and dissociation rate than QNB (Fig. 2, Table 3). However, the conformity of [^{3}H]NMS and [^{3}H]QNB saturation isotherms with the law of mass-action (Fig. 1) and the similarities in the displacement of [^{3}H]NMS and [^{3}H]QNB by several muscarinic drugs (Figs. 4–6, Table 3) suggest that, as in other tissues [7, 33], the subpopulation of [^{3}H]QNB binding sites labeled by [^{3}H]NMS in the iris does not represent different receptor subtypes but differences in binding to the same population of receptors.

One objective of this study was to determine the mAChR subtype(s) in the iris. In various tissues two pharmacologically distinct classes of mAChRs, M_1 and M_2, have been defined based on their affinity, high and low respectively, for pirenzepine [7–9]. However, recent genetic data as well as studies with the apparently cardioselective muscarinic antagonist AFDX-116 suggest the existence of additional classes of mAChRs [3–6, 10–12, 36–38].

In general, the M_1 subtype appears to be the major subtype in neuronal tissues including cerebral cortex, hippocampus and sympathetic ganglia, whereas the M_2 subtype appears to be more prevalent in peripheral effector organs such as heart, smooth muscle and exocrine glands [7–9, 31, 33, 39]. Previous studies conducted in this laboratory, which compared receptor occupancy, muscle contraction, inositol triphosphate release and myosin light chain phosphorylation, suggested that in the iris the mAChR-stimulated polyphosphoinositide response is mediated by receptors which pharmacologically more closely resemble the M_2 than the M_1 subtype [40]. However, the affinity of iris mAChRs for pirenzepine appears to be different from other M_2 receptors. Thus, while the mAChRs in the iris bound pirenzepine with an affinity that was ~10-fold lower

Table 3. Summary of muscarinic binding constants for rabbit iris microsomes determined by using [^{3}H]NMS and [^{3}H]QNB as ligands

Kinetic parameter	Displacer	Radioligand [^{3}H]NMS	Radioligand [^{3}H]QNB
K_D (pM)		240	39
B_{max} (pmol/mg protein)		0.67	1.09
Hill coefficient		1.0	0.94
K_{+1} (M^{-1} min^{-1})		1.19×10^9	2.26×10^7
K_i (nM)	Atropine	0.965	0.657
	Pirenzepine	102	127
	Pilocarpine	10,700	7,430
	(−)QNB	0.046	0.039
	(+)QNB	4.6	5.01
K_H (μM)	Carbachol	5.9	2.9
	Methacholine	1.4	4.1
	Oxotremorine	1.6	1.5

than that of M_1 cerebral cortex receptors, iris mAChRs displayed a binding affinity for pirenzepine which was higher than either the ileal or cardiac (K_i = 505 nM; [41]) M_2 receptors (Fig. 6, Table 2). mAChRs with an intermediate binding affinity for pirenzepine can also be found in bovine iris (R. E. Honkanen and A. A. Abdel-Latif, unpublished observations), and careful examination of the literature reveals that an intermediate binding affinity for pirenzepine has been observed in other tissues whose mAChRs are generally referred to as belonging to the M_2 subtype [7].

Studies with the newly developed pyridobenzodiazepinone, AFDX-116, also reveal receptor binding profiles that are somewhat inconsistent with the presently employed M_1 and M_2 subclassification system [38, 42]. AFDX-116 appears to be selective for the M_2 receptor subtype, binding M_2 receptors with a ~10- to 20-fold higher affinity than M_1 receptors [37, 38]. In addition, AFDX-16 is able to distinguish cardiac M_2 from other M_2 receptors (i.e. AFDX-116 binds cardiac M_2 receptors with a greater affinity than it does other M_2 receptors [38, 42, 43]). Comparison of the binding affinity of AFDX-116 for mAChRs in iris (K_i = 308 nM), heart (K_i = 90 mM) and cerebral cortex (M_1 subtype; K_i = 811 nM) reveals that iris mAChRs have an affinity for AFDX-116 which is lower than that of the M_1 subtype but higher than that of cardiac M_2 receptors [41]. This is opposite of the binding profile observed for pirenzepine (Fig. 6). Further, the intermediate binding affinity of iris mAChRs observed for both pirenzepine and AFDX-116 does not appear to be due to the presence of more than one subtype of mAChRs in the iris, i.e. unlike the curves observed for the binding of these antagonists in cerebral cortex microsomes, the binding curves obtained with iris microsomes were steep and in excellent agreement with a one-binding-site model (Fig. 6, Table 2; [41]).

Tissue specific differences in receptor affinity for pirenzepine and AFDX-116 have been reported [7, 38, 42, 44, 45], and the molecular basis underlying these differences remains to be determined. One possibility is that the microenvironment of the membrane associated with the receptor varies in different tissues; this may alter the drug–receptor binding. Alternatively, the physical structure of the receptor itself may vary in different tissues. The existence of three or more subtypes of mAChRs is supported by recent molecular studies as well as studies with AFDX-116 [36–38, 42]. Further, an "M_3" receptor subtype, identified recently via the isolation and expression of complementary DNA derived from the cerebral cortex of rats, binds pirenzepine with an affinity which is intermediate between that of the M_1 and M_2 subtypes [36]. It is possible that mAChRs in the iris, which is a rather unique smooth muscle arising from the neuroectoderm of the optic cup and not from mesenchymal cells [46], are more closely related to the "M_3" subtype reported very recently by Bonner *et al.* [36] than to either of the presently defined M_1 or M_2 subtypes. Clearly, pharmacological studies alone are not sufficient to demonstrate conclusively that the different binding states of mAChRs observed in the iris, ileum, and brain represent distinct proteins. However, the present data together with our studies and those of others with AFDX-116 and the more recent genetic findings indicate the existence of more than two types of mAChRs.

In conclusion, the present study shows that the [^{3}H]NMS and [^{3}H]QNB binding sites of rabbit iris microsomes display most of the properties expected for mAChRs in peripheral tissues. However, the mAChRs of the iris had an affinity for pirenzepine that was lower than that of cerebral cortex receptors but higher than that of M_2 ileal receptors. These findings suggest that at least three binding states of mAChRs exist and support the hypothesis that there are more than two subtypes of mAChRs.

Acknowledgements—This work is supported by NIH Grants EY-04387 and EY-04171 and by a National Research Service Award Postdoctoral Fellowship EY-06050 (R. E. H.). We wish to thank Dr. Robert Aronstam of the Medical College of Georgia for discussion and helpful comments on this manuscript. This is Contribution No. 1072 from the Department of Cell and Molecular Biology, Medical College of Georgia.

REFERENCES

1. T. J. Yorio, *J. ocular Pharmac.* **1**, 397 (1985).
2. I. H. Leopold and E. Duzman, *A. Rev. Pharmac. Toxic.* **26**, 401 (1986).
3. A. S. V. Burgen, *Trends pharmac. Sci.* (Suppl.: Muscarinic Receptors I) 1 (1984).
4. T. K. Harden, L. I. Tanner, M. W. Martin, N. Nakahata, A. R. Hughes, J. R. Helper, T. Evans, S. B. Masters and J. H. Brown, *Trends pharmac. Sci.* (Suppl.: Muscarinic Receptors II) 14 (1986).
5. S. K. Fisher and B. W. Agranoff, *J. Neurochem.* **48**, 999 (1987).
6. A. A. Abdel-Latif, *Pharmac. Rev.* **38**, 227 (1986).
7. R. Hammer, C. P. Berrie, N. J. M. Birdsall, A. S. V. Burgen and E. C. Hulme, *Nature, Lond.* **283**, 90 (1980).
8. M. Watson, H. I. Yamamura and W. R. Roeske, *Life Sci.* **32**, 3001 (1983).
9. R. Hammer and A. Giachetti, *Life Sci.* **31**, 2991 (1982).
10. T. Kubo, K. Fukuda, A. Mikami, A. Maeda, H. Takahashi, M. Mishini, T. Haga, K. Haga, A. Ichiyama, K. Kangawa, M. Kojima, H. Matsuo, T. Hirose and S. Numa, *Nature, Lond.* **323**, 411 (1986).
11. T. Kubo, A. Maeda, K. Sugimoto, I. Akiba, A. Mikami, H. Takahashi, T. Haga, K. Haga, A. Ichiyama, K. Kangawa, H. Matsuo, T. Horise and S. Numa, *Fedn Eur. Biochem. Soc. Lett.* **209**, 367 (1986).
12. E. G. Peralta, J. W. Winslow, G. L. Peterson, D. H. Smith, A. Ashkenazi, J. Ramachandran, M. I. Schimerlik and D. J. Capon, *Science* **236**, 600 (1987).
13. R. A. Akhtar and A. A. Abdel-Latif, *Biochem. J.* **224**, 291 (1984).
14. P. H. Howe, R. A. Akhtar, S. Naderi and A. A. Abdel-Latif, *J. Pharmac. exp. Ther.* **239**, 574 (1986).
15. A. A. Abdel-Latif, P. H. Howe and R. A. Akhtar, in *Mechanisms of Signal Transduction by Hormones and Growth Factors* (Eds. M. C. Cabot and W. L. McKeehan), p. 119. Alan R. Liss, New York (1987).
16. S. Y. K. Yousufzai and A. A. Abdel-Latif, *Prostaglandins* **28**, 399 (1984).
17. R. Lund-Karlsen, *Expl Eye Res.* **27**, 577 (1978).
18. Y. Kloog, D. S. Heron, A. D. Korczyn, D. I. Sachs and M. Sokolovsky, *Molec. Pharmac.* **15**, 581 (1979).
19. W. C. Taft, A. A. Abdel-Latif and R. A. Akhtar, *Biochem. Pharmac.* **29**, 2713 (1980).
20. J. B. Hutchins and J. G. Hollyfield, *Expl Eye Res.* **38**, 515 (1984).

21. S. Y. K. Yousufzai, R. E. Honkanen and A. A. Abdel-Latif, *Invest. Ophthal. vis. Sci.* **28**, 1630 (1987).
22. M. Bradford, *Analyt. Biochem.* **72**, 248 (1976).
23. H. I. Yamamura and S. H. Snyder, *Proc. natn. Acad. Sci. U.S.A.* **71**, 1725 (1974).
24. P. J. Munson and D. Rodbard, *Analyt. Biochem.* **107**, 220 (1980).
25. G. Scatchard, *Ann. N.Y. Acad. Sci.* **51**, 660 (1951).
26. A. V. Hill, *Biochem. J.* **7**, 471 (1913).
27. J. Munson, *J. Receptor Res.* **3**, 249 (1983).
28. F. Konno and I. Takayanagi, *Jap. J. Pharmac.* **38**, 91 (1985).
29. C. Akesson, C. Swanson and P. N. Patil, *Naunyn-Schmiedeberg's Archs Pharmac.* **322**, 104 (1983).
30. J. A. D. M. Tonnaer, M. A. Van Vugt, T. de Boer and J. S. de Graaf, *Life Sci.* **40**, 1981 (1982).
31. L. T. Potter, D. D. Flynn, H. E. Hanchett, D. L. Kalinoski, J. Luber-Narod and D. C. Mash, *Trends pharmac. Sci.* (Suppl.: Muscarinic Receptors I) 22 (1984).
32. W. Hoss and W. Messer, *Biochem. Pharmac.* **35**, 3895 (1986).
33. E. E. El-Fakahany, V. Ramkumar and W. S. Lai, *J. Pharmac. exp. Ther.* **238**, 554 (1986).
34. R. S. Aronstam, L. G. Abood and J. Baumgold, *Biochem. Pharmac.* **26**, 1689 (1977).
35. J. H. Brown and D. Goldstein, *J. Pharmac. exp. Ther.* **238**, 580 (1986).
36. T. I. Bonner, N. J. Buckley, A. C. Young and M. R. Brann, *Science* **237**, 527 (1987).
37. E. Giraldo, R. Hammer and H. Ladinsky, *Life Sci.* **40**, 833 (1987).
38. R. Hammer, E. Giraldo, G. B. Schiavi, E. Monferini and H. Landinsky, *Life Sci.* **38**, 1653 (1986).
39. P. Vanderheyden, G. Ebinger, J. P. De Backer and G. Vauquelin, *Life Sci.* **39**, 1517 (1986).
40. R. A. Akhtar, R. E. Honkanen, P. H. Howe and A. A. Abdel-Latif, *J. Pharmac. exp. Ther.* **243**, 624 (1987).
41. R. E. Honkanen and A. A. Abdel-Latif, *Molec. Cellular Biochem.* in press.
42. R. Micheletti, E. Montagna and A. Giachetti, *J. Pharmac. exp. Ther.* **241**, 628 (1987).
43. S. P. Duckles, H. I. Yamamura and V. Lee, *Life Sci.* **40**, 1507 (1987).
44. M. Watson, W. R. Roeske and H. I. Yamamura, *J. Pharmac. exp. Ther.* **237**, 419 (1986).
45. M. Waelbroeck, M. Gillard, P. Robberecht and J. Christophe, *Molec. Pharmac.* **30**, 305 (1986).
46. J. Nolte, in *Physiology of the Human Eye and Visual System* (Ed. R. E. Records), p. 217. Harper & Row, New York (1979).